THE ASTRONOMICAL JOURNAL VOLUME 91, NUMBER 2 FEBRUARY 1986

STAR-FORMATION RATES IN THE NUCLEI OF VIOLENTLY INTERACTING GALAXIES[a]

HOWARD A. BUSHOUSE[b),c)]
Department of Astronomy, University of Illinois, Urbana, Illinois 61801
Received 24 July 1985; revised 25 September 1985

ABSTRACT

Spectrophotometry has been obtained of the nuclear regions of a large sample of violently interacting spiral galaxies. The sample galaxies were chosen to include only those systems having tails, plumes, or other morphological features consistent with strong tidal interactions involving disk galaxies. The interacting galaxies are found to exhibit a wide range of nuclear optical emission-line strengths, but show a significantly higher overall level in both Hα emission-line equivalent width and luminosity than samples of field spirals observed in a similar fashion. While galaxy-galaxy interactions *can* lead to large nuclear star-formation bursts, this is not a ubiquitous phenomenon. A large fraction ($\sim 30\%$) of the nuclei show only weak or no detectable optical emission lines and are characterized by stellar absorption spectra of old, elliptical galaxy-like stellar populations, thus indicating little recent or continuing star-formation activity. These circumstances can occur even in instances where the nucleus of the other component has a large population of young stars. While exhaustion of a galaxy's gas supply during the later phases of interaction can account for post-burst systems, it cannot explain systems that have experienced no significant star-formation activity throughout the entire interaction process. Seyfert and low-ionization nuclei also are rare in violently interacting systems which, coupled with the large number of nuclei found to have little star-formation activity, suggests either an initial lack of near-nuclear gas or that gas is present but in inappropriate forms to support star formation or fuel nuclear activity. This could occur if the central regions of the galaxies were gas-free before the interaction began and there was no subsequent radial transport of raw materials from the more gas-rich disk areas to the nuclear regions.

I. INTRODUCTION

Galaxy-galaxy interactions are now recognized as an important evolutionary process in many extragalactic systems, being held responsible for large-scale star-formation bursts, Seyfert activity, and even QSO phenomena. Recent bursts of star formation have been shown to be consistent with the often unusual optical colors (Larson and Tinsley 1978; Sharp and Jones 1980), near-infrared color and 10μm luminosity excesses (Joseph *et al.* 1984; Cutri and McAlary 1985), and excess radio continuum emission (e.g., Sulentic 1976; Stocke 1978; Condon 1980; Hummel 1980, 1981; Condon *et al.* 1982) of paired and interacting galaxies. An investigation of a small sample of strongly interacting galaxies from the *Atlas of Peculiar Galaxies* (Arp 1966), however, has shown little evidence for extreme bursts of star formation in all systems (Bushouse and Gallagher 1984). While current star-formation rates were found to be high in some systems, most were characterized by nearly constant rates of star formation over the past few billion years.

Interacting galaxy systems may also be connected with more exotic forms of nuclear activity. It has been suspected for some time that Seyfert galaxies tend to occur preferentially in multiple and interacting systems (Adams 1977; Vorontsov-Velyaminov 1977; Simkin *et al.* 1980; Balick and Heckman 1982; Dahari 1984, 1985). Keel *et al.* (1985) and Dahari (1985), however, find a significant lack of Seyfert and low-ionization nuclei in very disrupted systems. QSOs also seem to appear preferentially in multiple galaxy systems (Hutchings *et al.* 1982; Stockton 1982; Arp 1983; Hutchings and Campbell 1983), and therefore it has been suggested that galaxy-galaxy interactions may be responsible for QSO phenomena as well.

[a] Research supported in part by the U.S. National Science Foundation through Grant No. AST-82-14127 to the University of Illinois.

[b] Current address: National Optical Astronomy Observatories, Kitt Peak, P.O. Box 26732, Tucson, AZ 85726.

[c] Guest Observer, Steward Observatory, University of Arizona.

Due to the numerous and complex physical processes that occur during collisions between galaxies, however, we still do not have a full understanding of the specific effects of galaxy-galaxy interactions. I have begun an observational investigation of violently interacting galaxies in order to better understand and quantify the effects that interactions have upon star-formation activity within the systems involved. This paper presents results of a spectrophotometric survey of the nuclear regions of a large sample of violently interacting galaxies. Other components of this project will include emission-line imaging, global H I properties, and radio continuum mapping.

II. THE OBSERVATIONS

a) Sample Selection

By relying on observed properties of interacting galaxies as a means of defining the basic types of processes that take place during collisions, we are sensitive to the choice of interacting-galaxy samples. For example, data in the literature on "interacting galaxies" often refer to systems in close physical proximity, with or without the interpenetrating mass distributions that are a prerequisite for strong collisional coupling between galaxies. Other samples are derived from the heterogeneous selection of disturbed systems in the *Atlas of Peculiar Galaxies* (Arp 1966) or the *Atlas and Catalogue of Interacting Galaxies* (Vorontsov-Velyaminov 1959, 1977). In this investigation the emphasis is upon pairs of galaxies that are not merely close to one another, but rather those which exhibit morphological features unmistakably associated with strong gravitational interactions. Candidate systems were selected based upon morphological descriptions from the *Uppsala General Catalogue of Galaxies* (Nilson 1973; hereafter referred to as UGC). In order to be accepted as a candidate for the sample, a double system must be described in the UGC as interacting, disrupted, or disturbed. On this basis

$\sim$400 interacting systems were chosen from the UGC for further examination.

Final selection of the sample was based upon visual inspection of each interacting system on the Palomar Sky Survey prints or other larger-scale photographs (e.g., the Arp *Atlas*). Only systems that have tails, plumes, rings, or other morphological features consistent with strong tidal interaction were included in the final sample, regardless of the physical separation of the galaxies, their relative sizes, or their environment. Since this is a morphologically selected sample, it is certainly incomplete in terms of sampling the full range of interaction strengths and galaxy luminosity.

The sample has also been limited to systems that show some evidence for the presence of stellar disks, either from the structure of undisturbed parts of galaxies, or as a natural consequence of selecting systems with strong tidal tails. As Toomre and Toomre (1972) pointed out in their classic modeling study of galaxy collisions, well-defined tidal tails are most readily produced by the disruption of stellar disk components of galaxies, and thus provide a means for finding disk systems even in severely disturbed galaxy pairs. Disk-type systems are preferred both for their higher gas content (and therefore ease of detecting star-formation activity) and for facilitating comparisons with similarly observed samples of isolated galaxies. These selection criteria yielded a final sample of $\sim$100 strongly interacting systems, selected without bias towards any *a priori* knowledge of other physical parameters such as optical colors, spectral characteristics, environment, or level of radio emission.

Numerical simulations of interacting galaxies help to reveal several biases that have been introduced into the sample by the selection criteria. First, these systems are being observed at late phases of the interaction, since it is known that severe morphological disturbances, such as long tidal tails, require $>10^8$ yr to develop (Toomre and Toomre 1972; Toomre 1977; White 1983; Smith and Miller 1982). Second, the presence of long tidal tails also indicates that the mass ratios of many of the galaxy pairs are near unity (e.g., Toomre and Toomre 1972). Finally, the majority of interacting galaxies in this sample do not reside in regions of high galactic density, since severe morphological disturbances of the kind selected for require slow, parabolic passages of the galaxies (cf. Toomre and Toomre 1972; Tremaine 1981). These are conditions not usually found in groups or clusters of galaxies, where the relative velocities are high.

b) Observational Procedures and Data Reduction

Low to moderate signal-to-noise ratio spectrophotometry has been obtained of the nuclear regions of 94 individual galaxies from the interacting sample. This includes observations of both galaxies in each of 25 pairs, and 44 individual galaxies belonging to separate multiple systems. The term "nuclear regions" is used, since the observations were obtained through moderately small (5 arcsec) apertures centered visually on the peak of the light distribution of each object as seen on a red-sensitive acquisition TV monitor (with some consideration given to the apparent location of the nucleus on the red POSS prints), and therefore the observations include both the true nucleus as well as varying amounts of the surrounding disk regions of the galaxies.

All observations were obtained with the Steward Observatory 2.3 m telescope, using the Cassegrain spectrograph and intensified photon-counting Reticon system. A 600 line mm^{-1} grating provided an effective wavelength coverage of 3650–6900 Å and a FWHM resolution of 8 Å. Total integration times for the majority of objects were 12 min. The spectrograph and detector is a dual-beam system, and therefore, when contamination of the second beam by the galaxy was negligible, sky subtraction was accomplished via beam switching between the two apertures. When the contribution of the galaxy to the sky beam was significant, the telescope was wobbled between the galaxy and a suitably chosen blank sky either north or south of the object. Observations each night of four or five standard stars from the lists of Oke (1974) and Filippenko and Greenstein (1984) provided the calibration to an absolute-flux scale. Comparison-lamp observations obtained at the same sky positions as the program objects were used to correct for zero-point drifts in the wavelength solution due to instrumental flexure. As a rule, these shifts were $\leqslant 0.7$ Å.

Observations made in January and April 1984 were obtained without the use of an order separation filter in the spectrograph, and therefore second-order blue light contributed to the observed spectra at wavelengths greater than $\sim$6300 Å. Since the observed standard stars have very blue optical colors, this led to an error in flux calibration above $\sim$6300 Å. The direction of the error is such that program objects show a drop in absolute flux at these wavelengths. Observations obtained in June and November 1984 do not suffer from this effect as an appropriate order-blocking filter was used in obtaining these observations. By comparing the relative flux levels of standard stars observed in both modes a correction factor was determined and applied to the emission-line fluxes for program objects observed in January and April. Emission-line equivalent widths are not affected by this problem.

Data reduction was performed on the University of Illinois VAX and Image Processing system (VIP), using the Steward Observatory Interactive Reduction System (IRS) installed on the VIP by C. Foltz. Standard reduction techniques yielded the fluxed spectra, which were subsequently corrected for Galactic reddening on the basis of extinction estimates from Burstein and Heiles (1982, 1984), using the Whitford (1958) extinction curve.

c) Data Analysis

Radial velocities were previously unknown for the majority of the systems observed. Therefore radial velocities were calculated for each of the galaxies from the observed wavelength shifts of the strongest emission and/or absorption lines in their spectra. A comparison with known radial velocities and also with measurements of night-sky lines shows the calculated velocities to be accurate to ± 150 km s^{-1}. Table I lists the program galaxies, observed radial velocities, and integrated apparent and absolute blue magnitudes. Apparent magnitudes are on the B_T system and were obtained (when available) from the *Second Reference Catalogue of Bright Galaxies* (deVaucouleurs, deVaucouleurs, and Corwin 1976; hereafter referred to as RC2), or from the UGC, and then converted to the B_T system following the methods of Fisher and Tully (1981). Absolute magnitudes are calculated from B_T and distances inferred from $H_0 = 75$ km s^{-1} Mpc^{-1} using the linear Hubble flow model of Schecter (1980) with a Virgo infall velocity of 250 km s^{-1}.

The spectra have been classified on the basis of relative strengths of prominent emission and absorption features, following the system employed by Arp (1982). Emission spectra are classified as follows:

TABLE I. Program galaxies.

UGC (1)	NGC (2)	Arp (3)	E(B-V) (4)	V_o (5)	D (6)	B_T (7)	M_B (8)	Date (9)
		256 S	.00	8094	84.4			1/84
248 S			.02	10416	109.8	14.6	-20.6	1/84
480 W			.04	11228	118.9	13.6:	-22.0:	1/84
480 E			.04	11128	117.8			1/84
		251 N	.00	22906	243.0			11/84
594	317 b		.10	5284	58.6	13.7	-20.1	11/84
717		11 a	.02	11154	117.5	14.0	-21.4	11/84
813			.12	5189	54.8	14.7	-19.5	1/84
816			.12	5529	58.5	14.4	-19.9	1/84
993 E			.04	3059	31.2	15.2	-17.3	11/84
1063	569 a		.05	5958	62.0	14.5	-19.7	1/84
1065	569 b		.05	5878	61.1	15.3	-18.7	11/84
1095 E		98 E	.04	12390	134.8	14.7	-20.9	11/84
1228 S			.06	4112	42.8	14.8	-18.6	1/84
1720 N			.03	9144	96.0	14.2:	-20.8:	11/84
1720 S			.03	8889	93.3			1/84
2320 N		190 N	.09	10128	106.9	14.9:	-20.6:	1/84
2320 S		190 S	.09	10068	106.2			1/84
2992 W			.12	4974	52.4	15.0:	-19.0:	1/84
2992 E			.12	5004	52.8			1/84
3031	1568 a		.06	4536	47.9	14.6	-19.0	1/84
3032	1568 b		.06	4636	48.9	14.1	-19.6	1/84
	1614		.06	4623	49.0	13.6	-19.8	11/84
3706 N			.08	6211	67.8	14.5:	-20.0:	1/84
3706 S			.08	6141	67.1			1/84
3737			.08	4392	48.5	14.9	-18.8	1/84
		250 W	.04	24181	260.2			4/84
		250 E	.04	24181	260.2			11/84
4264 N	2535	82 N	.04	3902	45.1	13.1	-20.3	11/84
4264 S	2536	82 S	.04	3952	45.2	14.7	-18.7	11/84
4509	2623	243	.02	5220	59.6	14.4	-19.6	11/84
4653 S		195 S	.02	16182	175.2	14.7	-21.6	1/84
4757	2744		.02	3272	38.3	13.8	-19.2	11/84
4881 W		55 W	.00	11634	126.6	14.6:	-20.9:	1/84
4881 E		55 E	.00	11694	127.3			1/84
		252 N	.07	9439	103.2			4/84
		252 S	.07	9429	103.1			4/84
5304 N		255 N	.01	11837	129.2	14.5:	-21.1:	1/84
5304 S		255 S	.01	12137	132.5			1/84
5367 N			.00	6911	76.5	15.2:	-19.2:	1/84
5367 S			.00	6991	77.3			1/84
5600			.00	2792	32.0	14.2	-18.3	1/84
5609			.00	2762	31.7	14.3	-18.2	1/84
5643	3212	181	.00	9837	106.7	14.1	-21.0	1/84
5938			.01	10580	114.8	15.5	-19.8	1/84
5942			.01	10789	117.0	15.9	-19.5	1/84
6264 N	3588 N		.00	7948	88.2	14.9:	-19.8:	1/84
6264 S	3588 S		.00	7968	88.4			1/84
6527 a		322 a	.00	7950	87.6			4/84
6527 d		322 d	.00	7930	87.4	14.5	-20.3	4/84
6748			.00	10604	116.4	15.5	-19.8	4/84
6865 N		62 N	.00	5943	66.6	14.5:	-19.7:	1/84
6865 S		62 S	.00	5693	64.0			1/84
7070			.00	2663	31.8	15.0	-17.5	1/84
7085A N		97 N	.00	6892	77.0	14.8:	-19.7:	1/84
7085A S		97 S	.00	6792	75.9			1/84
7230		260	.03	7068	79.0	14.5	-20.1	1/84
7891 N			.02	7024	78.4	15.1:	-19.4:	1/84
7891 S			.02	7069	78.9			1/84
7905 N			.01	5024	56.6	14.0:	-19.8:	4/84
7905 S			.01	5064	57.0			4/84
7910			.00	3623	42.2	15.0	-18.1	1/84
7936 N			.00	7475	82.9	14.9:	-19.7:	1/84
7936 S			.00	7425	82.3			1/84
8315			.00	1195	18.0	15.2	-16.1	4/84
8335		238	.01	9222	100.9	14.2	-20.8	1/84
8357			.01	9814	108.1	14.3	-20.9	1/84
8416			.00	8922	98.0	15.2	-19.8	1/84
8454 E		204 E	.08	6444	70.4	15.2	-19.4	4/84
8584 S			.01	17291	188.0	15.0	-21.4	1/84
8774 N	5331 a		.01	9651	106.3	14.1	-21.0	1/84
8849 N			.00	6344	71.1	14.5	-19.7	4/84
8929			.01	8239	91.2	14.8	-20.1	1/84
8931	5410		.00	3780	43.8	14.0	-19.2	1/84
9001			.00	11186	122.7	14.8	-20.7	4/84
9102 N	5514 N		.01	7131	79.4	13.9	-20.7	1/84
9178 N		45 N	.00	8818	96.8	15.1	-19.8	4/84
9326			.03	15916	173.1	15.1	-21.2	4/84
9507	5755	297	.00	9692	106.3	14.2	-20.9	4/84
9580			.01	8793	96.8	14.9	-20.0	4/84
10610 W			.00	10116	109.9	14.7:	-20.5:	4/84
10610 E			.00	9996	108.6			6/84
10770 S		32 S	.01			14.1		4/84
10923 W			.05	8029	87.1	14.1	-20.8	4/84
11044			.09	3066	34.4	14.7	-18.3	4/84

TABLE I. (continued)

UGC (1)	NGC (2)	Arp (3)	E(B-V) (4)	V_o (5)	D (6)	B_T (7)	M_B (8)	Date (9)
11284 W	6670 W		.05	8510	92.1	14.9:	-20.1:	6/84
11284 E	6670 E		.05	8790	95.1			4/84
11695			.05	9553	104.5	14.5	-20.6	11/84
12066 E			.05	5871	61.4	14.4	-19.6	11/84
12099	7318 a	319 a	.08	6879	73.5	14.3	-20.0	6/84
12589			.03	10166	106.7	15.2	-20.0	11/84
12911	7806	112 b	.04	5069	53.0	14.2	-19.4	11/84
12914			.04	4614	47.8	12.7	-20.7	11/84
12915			.04	4024	49.4	13.8	-19.7	11/84

Notes:

Col. (1)-(3) Galaxy identification from the UGC, NGC, and Arp *Atlas*.

Col. (4) Color excess due to Galactic reddening, determined from Burstein and Heiles (1984).

Col. (5) Observed radial velocity, in km s^{-1}, corrected for solar motion relative to the centroid of the Local Group.

Col. (6) Distance, in Mpc, computed using the linear Hubble flow model of Schecter (1980) with a Virgo infall velocity of 250 km s^{-1} and H_o=75 km s^{-1} Mpc^{-1}.

Col. (7) Total apparent B magnitude taken from the RC2, or m_b taken from the UGC and transformed onto the B_T system according to Fisher and Tully (1982). A ':' indicates that the value listed is the combined magnitude of both galaxy components.

Col. (8) Absolute B magnitude, calculated using D from Col. (6) and B_T from Col. (7) after correcting for external reddening using E(B-V) from Col. (4) and A_B=4.1*E(B-V).

Col. (9) Date of observation.

(0) No detectable emission lines.
(1.5) [O II] λ 3727 emission only.
(2.0) [O II], Hβ, [O III] $\lambda\lambda$ 4959 + 5007, and Hα emission dominant.
(2.5) H II region-like, including all of the above features plus [Ne III] $\lambda\lambda$ 3868 + 3967 and [N II] $\lambda\lambda$ 6548 + 6584.
The continuum classifications are:
(0) Unclassifiable, due to either insufficient signal-to-noise, or a featureless H II region-like continuum.
(1) Old elliptical galaxy-like stellar spectrum dominated by Ca II H and K, *G* band, Mg I, and Na D absorption features.
(1.5) Intermediate-age, composite spectrum including Ca II, *G* band, and Hβ absorption.
(2.0) Dominant hydrogen Balmer-line absorption.
Intermediate classifications (e.g., 1.7, 2.2) were assigned when spectral features belonging to more than one class were present at approximately equal strengths. Typical examples of each class are shown in Fig. 1.

Emission-line fluxes were measured by fitting the features with simple Gaussians using an interactive spectral-analysis program developed on the University of Illinois VIP. Observations of a few objects on more than one night show the measured line fluxes to be consistent to ~20%. Table II lists the dereddened emission-line fluxes, as well as the projected aperture diameter (in kpc) and the spectral class of each of the observed systems.

III. RESULTS

a) Spectral Classification

We expect that nuclei that are currently experiencing star-formation bursts will have H II region-like spectral characteristics, while those in a post-burst phase will be dominated by intermediate-age A-type stellar spectra. Surveys of large samples of isolated galaxies suggest that noninteracting galaxies with A-type spectra are relatively rare, accounting for no more than ~10% of all systems (e.g., Morgan and Mayall 1957; Morgan 1958; Morgan 1959; Heckman, Balick, and Crane 1980). The most striking result of the spectral classification of the interacting galaxies studied here is the large fraction (~30%) of systems that are similar to elliptical galaxies, dominated by an old population of G–K type stars (continuum class 1). These systems show no sign of significant star-formation activity at any time in their recent past histories. If we expect that violent interactions will commonly lead to large-scale nuclear star-formation bursts, it is indeed surprising to find such a large fraction of systems with no continuing star-formation activity in their nuclear regions. Approximately 20% of the interacting systems do have Balmer absorption-line spectra (continuum class 2) and are therefore assumed to be in a post-burst phase. The remaining systems have either featureless or unclassifiable continuum spectra (class 0) or belong to the intermediate category (class 1.5).

The distribution of emission spectra follows the same pattern. I find that a little more than 20% of the interacting galaxies have emission features characteristic of conventional H II regions (class 2.5), while more than 30% show either no detectable emission lines or [O II] λ 3727 emission only (class 0 to 1.5). The remaining systems ($\gtrsim$40%) fall into the intermediate category (class 2.0), and are dominated by [O II], Hβ, [O III], and Hα emission. Furthermore, there is an almost one-to-one correspondence between the emission and absorption classes for individual objects. Those galaxies with little or no detectable emission (class 0 to 1.5) are almost always dominated by an old stellar absorption spectrum (class 1.0), while those with stronger emission features (class 2.0 to 2.5) also have absorption spectra characteristic of younger stellar populations (class 1.5 to 2.0).

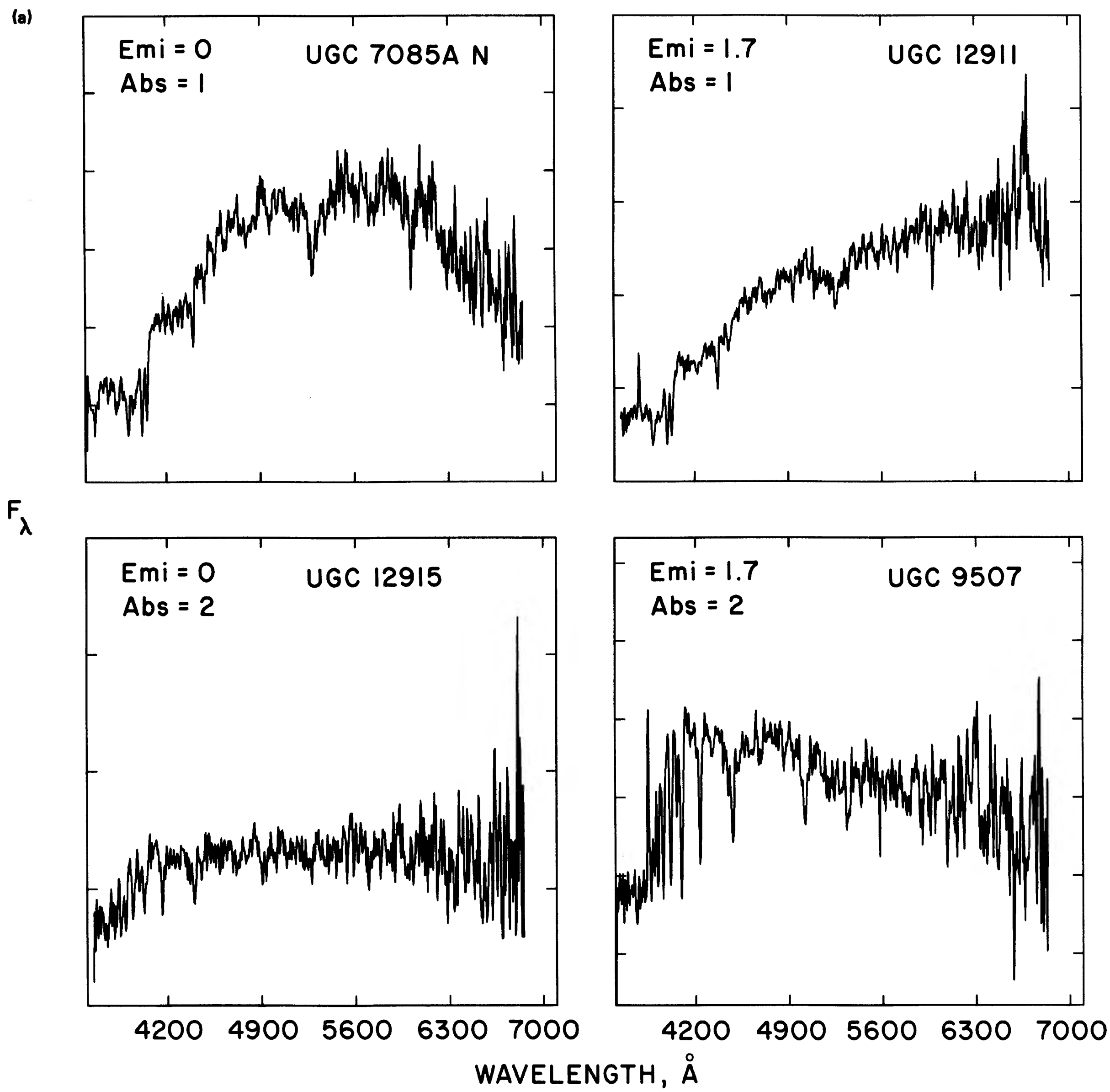

FIG. 1. (a) Representative spectra of nuclei with either no detectable emission lines (UGC 7085A N and UGC 12915) or weak emission lines (UGC 12911 and UGC 9507). Spectra are on a relative F_λ scale. Emission and absorption classifications are shown. UGC 7085A N and UGC 12911 both have late-type absorption spectra (class 1.0), while UGC 12915 and UGC 9507 have Balmer-line absorption features characteristic of intermediate-age A–F type stars. Note the downward turn in flux longward of ~6300 Å in the spectrum of UGC 7085A N due to the calibration errors discussed in Sec. II*b*.

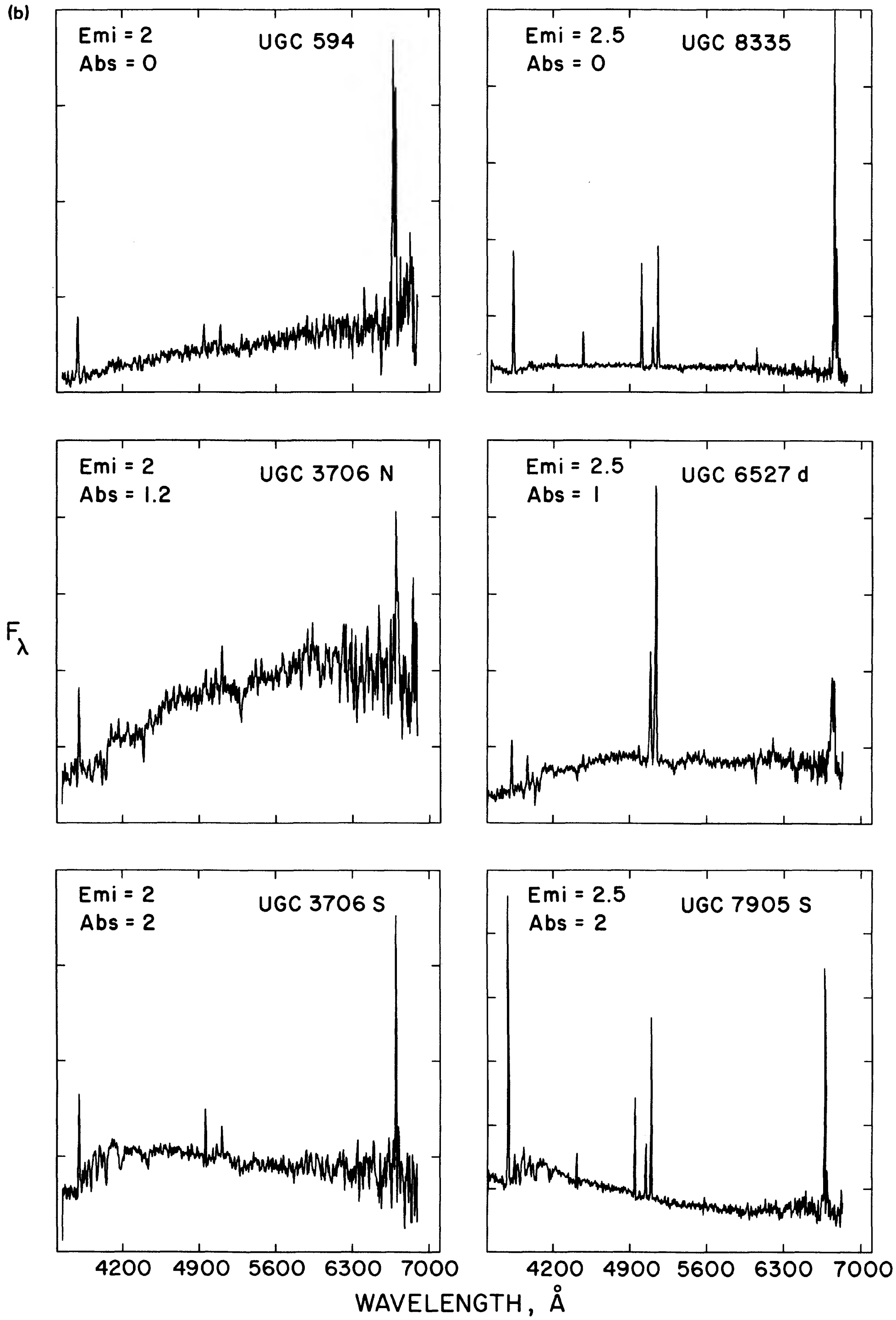

FIG. 1. (b) Representative spectra of nuclei with H II region emission superposed upon various types of absorption spectra. Spectra are on a relative F_λ scale. Emission and absorption classifications are shown. UGC 594 (also a LINER candidate) and UGC 8335 have featureless continua of absorption class 0. UGC 3706 N and UGC 6527d (the only Seyfert nucleus in the sample) show the superposition of H II region emission and late-type absorption spectra, while UGC 3706 S and UGC 7905 S show H II region emission superposed upon A–F type stellar spectra.

TABLE II. Emission data.

UGC	NGC	Arp	Aper.	Emi. Class	Abs. Class	F(Hα)	W_λ(Hα)	[OII] λ3727	Hγ λ4340	Hβ λ4861	[OIII] λ4959	[OIII] λ5007	[NII] λ6583
(1)	(2)	(3)	(4)	(5)	(6)	(7)	(8)	(9)	(10)	(11)	(12)	(13)	(14)
		256 S	2.0	2.5	0.0	145.	1090.	38.5	9.30	26.7	6.34	18.9	51.5
248 S			2.7	1.5	1.2	< 4.5	< 18.	2.06	-----	-----	-----	-----	-----
480 W			2.9	1.0	1.0	< 4.6	< 5.1	3.06	-----	-----	-----	-----	-----
480 E			2.9	0.0	1.0	< 4.0	< 5.7	-----	-----	-----	-----	-----	-----
		251 N	5.9	2.0	1.2	-----	-----	4.82	0.54	1.51	-----	1.12	-----
594	317 b		1.4	2.0	0.0	41.2	60.5	10.6	-----	4.73	-----	3.45	29.2
717		11 a	2.8	0.0	1.0	< 4.7	< 8.2	3.39	-----	-----	-----	-----	-----
813			1.3	2.2	1.7	50.8	49.2	19.3	-----	10.6	< 2.83	4.06	19.2
816			1.4	2.0	1.5	63.4	193.	14.2	-----	10.6	-----	2.98	31.1
993 E			0.8	2.5	0.0	24.4	566.	12.0	2.17	6.74	5.63	18.2	< 1.61
1063	569 a		1.5	2.0	2.0	24.9	29.1	7.87	-----	3.88	< 2.22	2.85	12.1
1065	569 b		1.5	2.2	1.7	12.8	370.	9.05	0.93	2.16	1.35	3.64	< 2.59
1095 E		98 E	3.3	2.0	1.2	20.2	41.8	3.76	-----	9.06	-----	< 0.81	10.1
1228 S			1.0	2.0	1.2	15.2	345.	11.4	-----	2.86	2.21	4.93	< 2.55
1720 N			2.3	2.0	1.7	10.6	215.	2.57	-----	1.05	-----	1.16	5.37
1720 S			2.3	2.5	1.7	104.	201.	28.8	5.62	21.8	6.10	21.3	53.9
2320 N		190 N	2.6	1.5	0.0	< 4.0	< 58.	2.34	-----	-----	-----	-----	-----
2320 S		190 S	2.6	0.0	1.2	< 5.1	< 16.	-----	-----	-----	-----	-----	-----
2992 W			1.3	2.5	0.0	167.	1610.	82.2	18.3	49.6	49.9	147.	28.4
2992 E			1.3	2.0	2.0	33.0	132.	6.00	-----	4.64	-----	3.33	14.1
3031	1568 a		1.2	2.0	1.5	21.4	123.	2.88	-----	2.88	-----	1.40	12.4
3032	1568 b		1.2	1.0	1.0	< 7.8	< 3.1	7.75	-----	-----	-----	-----	-----
	1614		1.2	2.5	0.0	811.	164.	62.2	27.6	92.8	21.8	70.0	464.
3706 N			1.6	2.0	1.2	< 5.0	< 8.4	8.42	-----	2.51	-----	2.84	-----
3706 S			1.6	2.0	2.0	28.0	39.2	10.2	-----	4.84	-----	5.80	< 2.80
3737			1.2	2.5	1.7	49.7	126.	43.8	-----	10.9	14.6	37.2	< 2.54
		250 W	6.3	1.5	1.5	-----	-----	3.16	-----	-----	-----	-----	-----
		250 E	6.3	0.0	0.0	-----	-----	-----	-----	-----	-----	-----	-----
4264 N	2535	82 N	1.1	2.0	1.7	54.7	40.1	4.47	-----	8.23	-----	< 1.18	28.4
4264 S	2536	82 S	1.1	2.0	1.7	6.53	6.4	11.2	-----	< 1.29	-----	3.09	6.78
4509	2623	243	1.4	2.0	1.7	18.5	15.8	5.09	-----	-----	-----	5.28	24.6
4653 S		195 S	4.3	2.2	1.2	-----	-----	11.9	-----	2.49	-----	1.92	-----
4757	2744		0.9	2.5	1.7	122.	132.	54.8	8.09	22.7	9.73	28.6	40.5
4881 W		55 W	3.1	1.7	1.5	< 4.0	< 16.	2.91	-----	-----	-----	-----	-----
4881 E		55 E	3.1	1.5	1.7	< 5.1	< 20.	3.51	-----	0.95	-----	-----	-----
		252 N	2.5	2.5	0.0	243.	393.	65.3	18.9	49.7	29.4	82.6	94.8
		252 S	2.5	2.0	0.0	< 4.6	< 15.	14.8	-----	5.68	< 1.74	2.90	-----
5304 N		255 N	3.1	2.5	1.7	36.2	134.	18.7	3.77	12.8	4.98	13.3	-----
5304 S		255 S	3.2	0.0	1.0	< 1.4	< 6.4	-----	-----	-----	-----	-----	-----
5367 N			1.9	2.5	0.0	27.9	1560.	13.6	1.84	4.20	1.75	5.40	6.63
5367 S			1.9	2.0	1.2	< 3.3	< 46.	5.54	-----	1.05	-----	2.23	-----
5600			0.8	2.5	1.7	340.	134.	41.7	15.9	46.5	9.28	25.8	126.
5609			0.8	2.2	2.0	14.3	90.0	8.77	-----	1.41	-----	5.65	< 1.08
5643	3212	181	2.6	1.0	2.0	< 5.8	< 6.5	2.56	-----	-----	-----	-----	-----
5938			2.8	2.2	1.5	14.7	94.1	6.49	0.54	3.76	-----	2.10	-----
5942			2.8	2.0	1.5	< 3.0	< 23.	3.57	-----	1.79	-----	< 2.38	-----
6264 N	3588 N		2.1	2.0	1.5	26.8	56.1	4.98	5.73	1.34	0.83	2.58	10.4
6264 S	3588 S		2.1	1.2	1.0	< 6.3	< 4.7	3.21	-----	-----	-----	-----	-----
6527 a		322 a	2.1	2.0	2.0	< 4.7	< 7.3	4.70	-----	1.73	-----	-----	-----
6527 d		322 d	2.1	2.5	1.0	104.	25.4	32.5	-----	8.18	80.3	206.	92.8
6748			2.8	1.7	1.5	< 3.8	< 33.0	4.38	-----	1.41	-----	-----	-----
6865 N		62 N	1.6	1.7	1.0	< 5.5	< 6.9	-----	-----	-----	-----	-----	-----
6865 S		62 S	1.5	2.0	2.0	18.6	36.3	6.28	-----	3.77	-----	0.81	13.7
7070			0.8	1.7	1.5	10.9	186.	3.80	-----	0.54	1.35	2.78	< 0.53
7085A N		97 N	1.9	0.0	1.0	< 3.7	< 4.8	-----	-----	-----	-----	-----	-----
7085A S		97 S	1.8	2.2	1.2	74.2	144.	17.0	2.82	9.63	< 3.54	4.91	50.9
7230		260	1.9	1.7	1.5	< 4.6	< 27.	5.45	-----	1.22	-----	-----	-----
7891 N			1.9	2.2	1.5	24.3	479.	17.7	-----	5.14	4.56	15.6	7.76
7891 S			1.9	2.5	2.0	14.1	90.3	11.1	2.63	1.71	1.33	6.49	< 2.37
7905 N			1.4	2.2	2.0	59.1	81.1	42.5	4.27	9.16	9.97	29.4	4.94
7905 S			1.4	2.5	2.0	163.	68.8	139.	32.2	40.8	24.2	72.8	33.6
7910			1.0	2.5	1.7	10.4	141.	5.58	0.68	1.94	4.48	11.8	< 1.44
7936 N			2.0	2.5	2.0	34.1	90.0	20.0	1.83	6.02	2.12	6.47	8.73
7936 S			2.0	2.5	0.0	16.2	462.	16.9	2.97	6.07	4.82	14.1	< 0.28
8315			0.4	2.5	0.0	113.	1090.	79.4	17.0	35.2	55.8	167.	< 4.66
8335		238	2.5	2.5	0.0	313.	231.	77.2	17.3	53.3	20.5	56.3	126.
8357			2.6	2.5	1.7	73.9	134.	13.4	17.7	9.35	1.69	7.44	25.8
8416			2.4	1.5	1.0	< 7.0	< 5.4	8.60	-----	-----	-----	3.26	-----
8454 E		204 E	1.7	2.5	2.0	98.1	381.	58.2	9.32	24.2	19.1	54.3	32.5
8584 S			4.6	2.0	1.5	-----	-----	15.9	2.76	11.5	< 2.51	5.09	-----
8774 N	5331 a		2.6	1.7	1.2	35.3	16.3	7.72	-----	3.33	-----	4.16	8.11
8849 N			1.7	1.5	1.2	< 5.0	< 4.5	4.95	-----	-----	-----	-----	-----
8929			2.2	2.5	2.0	33.8	37.3	28.6	3.07	9.92	4.42	11.6	13.4
8931	5410		1.1	2.2	2.0	17.9	17.2	10.5	-----	11.1	-----	2.06	< 1.83
9001			3.0	2.0	1.7	31.5	133.	12.1	-----	5.52	-----	3.01	< 5.22
9102 N	5514 N		1.9	1.5	1.0	< 9.6	< 9.3	7.03	-----	-----	-----	-----	-----
9178 N		45 N	2.3	2.0	1.7	17.6	69.4	6.72	1.55	4.29	-----	< 0.95	5.98
9326			4.2	1.5	1.5	< 3.1	< 5.5	2.59	-----	-----	-----	-----	-----
9507	5755	297	2.6	1.7	2.0	< 4.5	< 5.2	-----	-----	-----	-----	-----	-----
9580			2.3	2.0	1.2	< 2.8	< 11.	6.16	-----	1.78	0.99	2.87	-----
10610 W			2.7	2.2	1.5	24.5	33.4	6.28	2.96	6.30	1.10	3.00	6.80
10610 E			2.6	1.0	1.2	< 2.6	< 3.7	1.54	-----	8.41	-----	-----	-----
10770 S		32 S	0.0	2.0	2.0	< 3.1	< 21.	-----	-----	-----	-----	-----	-----
10923 W			2.1	2.0	1.7	77.2	41.8	6.67	-----	9.02	-----	2.57	18.1
11044			0.8	2.0	1.7	< 4.7	< 16.	10.1	-----	1.50	< 1.88	4.16	-----
11284 W	6670 W		2.2	2.2	1.7	45.0	166.	7.30	1.11	6.35	-----	2.10	20.3
11284 E	6670 E		2.3	2.2	1.7	81.8	73.5	11.9	-----	11.2	-----	7.18	18.5
11695			2.5	2.0	1.2	7.62	10.9	3.69	-----	2.33	-----	-----	< 1.38
12066 E			1.5	2.2	1.7	41.8	84.0	22.9	2.67	9.33	2.70	7.86	16.6
12099	7318 a	319 a	1.8	0.0	1.0	13.7	3.6	-----	-----	-----	-----	-----	-----

TABLE II. (continued)

UGC	NGC	Arp	Aper.	Emi. Class	Abs. Class	F(Hα)	W_λ(Hα)	[OII] λ3727	Hγ λ4340	Hβ λ4861	[OIII] λ4959	[OIII] λ5007	[NII] λ6583
(1)	(2)	(3)	(4)	(5)	(6)	(7)	(8)	(9)	(10)	(11)	(12)	(13)	(14)
12589			2.6	1.7	1.5	11.8	25.5	3.82	-----	< 4.80	-----	1.27	< 1.33
12911	7806	112 b	1.3	1.7	1.0	17.3	4.8	9.85	-----	-----	-----	4.48	19.0
12914			1.2	2.0	1.0	34.1	12.1	8.11	-----	11.0	-----	2.67	35.3
12915			1.2	0.0	2.0	< 3.5	< 8.4	-----	-----	< 12.5	-----	-----	-----

Notes:

Col. (1)-(3) Galaxy identification from the UGC, NGC, and the Arp *Atlas*.

Col. (4) Projected aperture diameter, in kpc, computed using distance in Table I.

Col. (5) Spectral emission classification.

Col. (6) Spectral absorption classification.

Col. (7) Observed Hα emission flux, corrected for Galactic reddening, in units of 10^{-15} ergs cm^{-2} s^{-1}.

Col. (8) Observed Hα equivalent width, in Å.

Col. (9)-(14) Observed emission line fluxes, corrected for Galactic reddening, in units of 10^{-15} ergs cm^{-2} s^{-1}.

b) Ionization Mechanisms

For the interacting systems that have detectable emission features it is important to determine the physical mechanisms responsible for excitation of the emitting gas. The use of line-ratio diagrams, as introduced by Baldwin, Phillips, and Terlevich (1981), can effectively separate conventional H II region emission (i.e., photoionization by hot stars) from that attributed to either Seyfert activity (photoionization by a strong power-law continuum), shock excitation, or low-ionization nuclear emission regions (LINERs; Heckman 1980). It is not clear at this time whether LINERs are simply an extension of Seyfert 2s and are therefore energized by low-luminosity power-law sources, or are powered by shocked-heated gas (see for example Heckman 1980; Stauffer 1982; Ferland and Netzer 1983; Halpern and Steiner 1983; Keel 1983b; Osterbrock and Dahari 1983).

The basic diagnostic diagram plots the emission-line ratio [O III] λ 5007/Hβ vs [N II] λ 6583/Hα, and is shown in Fig. 2 for the interacting-galaxy data set. The adopted domains of H II, Seyfert, and LINER nuclei are those generally agreed upon by other authors (e.g., Baldwin, Phillips, and Terlevich 1981; Shuder and Osterbrock 1981; Keel *et al.* 1985). An object with [O III]/Hβ $\gtrsim$ 3.0 and [N II]/Hα $\gtrsim$ 0.7 is classified as a Seyfert nucleus. Objects that have [N II]/Hα $\gtrsim$ 0.7 but [O III]/Hβ $\lesssim$ 3.0 are assumed to be LINERs. The remaining nuclei are classified as H II regions.

It is evident from Fig. 2 that the vast majority of interacting galaxies that have detectable nuclear emission features are of the H II region variety and therefore represent normal star-formation activity. Few of the nuclei (10%–15%) can be classified as LINERs. Furthermore, out of more than 90 interacting galaxies surveyed, only one was found to contain a Seyfert nucleus (UGC 6527d = Mrk 176). Table III lists the galaxies that appear to be Seyfert or LINER-like. The almost one-to-one correspondence between stellar and emission spectral classes as discussed in the previous section further supports the conclusion that hot stars provide the majority of the power involved in exciting the observed emission regions. It would appear, therefore, that any long-lived optically detectable "activity" which might be generated by a collision between galaxies preferentially manifests itself in the form of star bursts in the later phases being observed here.

There exists a clear deficiency of "active" (i.e., Seyfert or LINER-like) nuclei within the sample of violently interacting galaxies when compared to samples of isolated disk galaxies, a result that is in agreement with both Keel *et al.* (1985) and Dahari (1985). LINERs show a clear preference for disk galaxies of early Hubble subtype, occurring in as many as 80% of isolated Sa and Sb galaxies, and account for at least ~20% of isolated Sc galaxies (Keel 1983a, 1985). Depending on morphological subtype, Seyfert nuclei are seen in ~5% of isolated disk galaxies (Keel 1983a; Phillips, Charles, and Baldwin 1983), although this figure is at present somewhat uncertain (see the recent review by Osterbrock 1985). Compare these values for isolated galaxies with the present survey of violent interactors, of which <15% are LINERs and ~1% are obvious Seyfert galaxies.

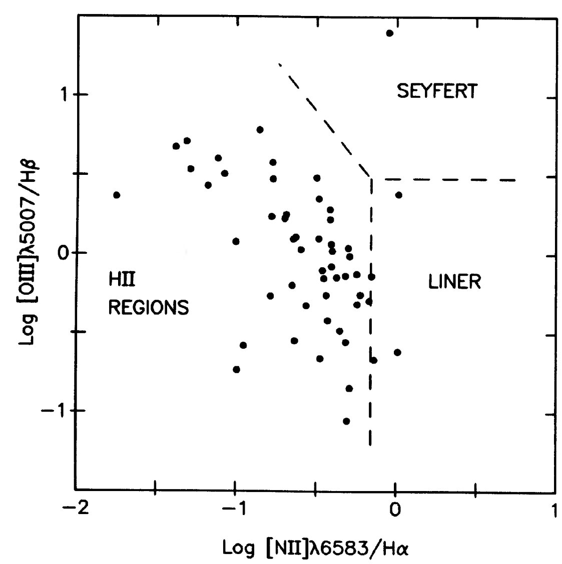

FIG. 2. Line ratio diagram [O III] λ 5007/Hβ vs [N II] λ 6583/Hα for the interacting galaxy nuclei, from which emission-line classifications were determined. The adopted boundaries of the classes are shown by dashed lines.

TABLE III. Seyfert and LINER nuclei.

Galaxy	Type	[N II]/Hα	[O III]/Hβ
UGC 594	LINER ?	0.71	0.73
UGC 4264 S	LINER	1.04	> 2.4
UGC 4509	LINER	1.33	—
UGC 6527d	Seyfert	0.89	25.2
UGC 6865 S	LINER ?	0.74	0.22
UGC 12911	LINER	1.10	—
UGC 12914	LINER	1.04	0.24

c) Emission-line Strengths

Measurement of the integrated Balmer photon flux in a galaxy provides a direct estimate of the Lyman continuum luminosity and the corresponding OB star-formation rate. The stellar continuum light at Hα wavelengths, meanwhile, is dominated by G–K giants. The Hα emission-line equivalent width, which is the ratio of integrated Hα emission to stellar continuum flux, is therefore also a measure of the ratio of the current to the average recent-past star-formation rate in a galaxy (e.g., Huchra 1977; Kennicutt 1983). A comparison, therefore, of the observed Hα equivalent widths in the sample of interacting galaxies with otherwise normal isolated disk galaxies will indicate the degree to which nuclear star formation is enhanced by the interaction process. It is possible, however, that in some systems the nucleus is heavily obscured by dust, which may preferentially affect the strength of the Hα emission. Thus optically measured Hα equivalent widths and luminosities are only lower limits.

There exist two major spectrophotometric surveys of the nuclei of isolated disk galaxies with which the data from the present survey may be compared. First, Stauffer (1982) has observed a sample of field spiral galaxies that were chosen from both Balkowski's (1973) list of galaxies observed in the H I 21-cm line and the galaxies in the *Hubble Atlas* (Sandage 1961) brighter than $B_T = 13.0$. Second, Keel (1983a) observed a statistically complete sample of spiral galaxies chosen from the RC2 with $B_T < 12.0$. I have eliminated objects in these control samples that might be construed as interacting with a nearby companion (e.g., M51). Heckman, Balick, and Crane (1980) have also observed a large sample of isolated galaxies in similar fashion. However, spectrophotometry in the wavelength region of Hα was obtained for only nine disk-type galaxies. In light of this rather small sample size, no direct comparisons will be made between their data and the interacting galaxies observed here.

The distributions of Hα equivalent width for the Stauffer and Keel samples of isolated spirals (hereafter referred to as the "control" sample) and for the interacting sample are shown in Fig. 3, and Table IV lists median values for several properties. The control samples possess median Hα emission-line equivalent widths of ~6 and ~8 Å, respectively. The sample of violently interacting galaxies studied here exhibits a large range in Hα equivalent width, from less than ~5 Å to more than 1000 Å, with a median W_λ (Hα)≃40 Å (Fig. 3). Only two of the nuclei in which Hα emission was not detected have estimated upper limits greater than this median value. Therefore eliminating these two values would have little effect upon the computed median. A Kolmogorov-Smirnov test shows the excess in Hα equivalent width of the interacting sample to be significant above the 99.9% level. It seems clear, therefore, that the central regions of many vio-

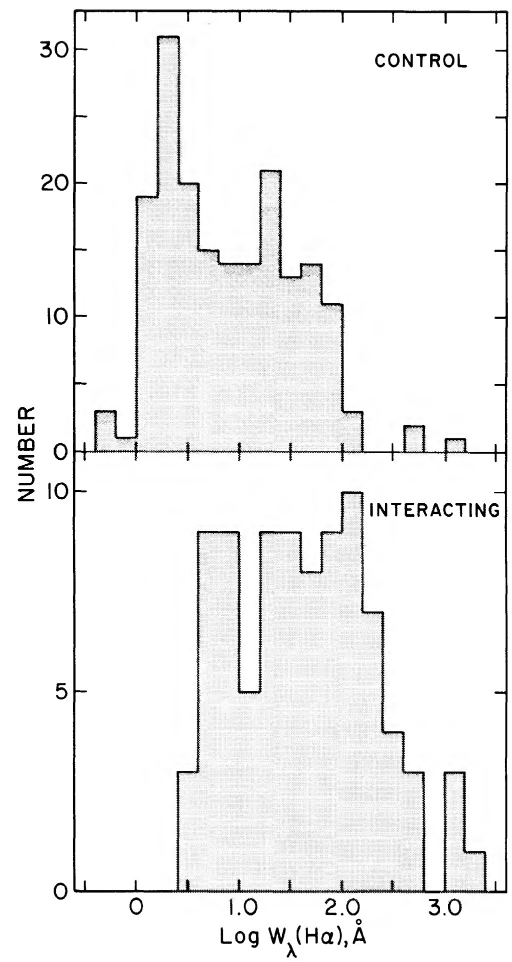

FIG. 3. Distribution of Hα equivalent widths for the interacting and combined isolated-galaxy samples.

TABLE IV. Median properties of galaxy samples.

	Present survey	Stauffer isolated	Keel isolated	Keel *et al.* "Complete"	Keel *et al.* "Arp"
M_B	− 19.8	− 20.1	− 19.7	− 19.6	− 20.2
cz (km s^{-1})	7475	1147	1230	1730	4900
Aperture (kpc)	2.01	< 0.6[a]	0.65	0.53	1.49
W_λ (Hα) (Å)	40	6	8	28	24
log L (Hα) (ergs s^{-1})	40.0	—[b]	38.5	39.0	40.2

[a] Several aperture sizes used, but not individually listed. Upper limit calculated using largest size quoted.
[b] Hα emission fluxes not given.

lently interacting galaxies are much more "bursty" in nature than isolated galaxies.

Similar results are obtained when the Hα emission-line luminosities of the interacting and control samples are compared (Fig. 4). The violently interacting systems have a median log L (Hα)$\simeq$40.0, while the median Hα luminosity for the Keel sample of isolated galaxies is more than a factor of 30 lower [log L (Hα)$\simeq$38.5]. (Hα fluxes were not published for the Stauffer survey). Again, a Kolmogorov-Smirnov test shows an excess in emission for the interacting sample with significance levels exceeding 99.9%. Note also that the Hα luminosities measured for many of the systems in the interacting sample may be only lower limits due to contamination by underlying stellar absorption and obscuration by dust. Keel's data for isolated spirals have been corrected for the effects of stellar absorption.

When making direct comparisons of this type we must of course be careful to consider any statistical biases that may occur as a result of observational selection. Since violently interacting galaxies are somewhat rare, the selection is naturally limited to objects that are on the average fainter and more distant than those in the control samples. Artificial differences between the samples then could arise from three effects. First, it is known that nuclear activity correlates in a positive sense with galaxian luminosity in spirals (cf. Keel 1985; Osterbrock 1985). A comparison of the distributions in absolute magnitude (scaled to $H_0 = 75$ km s^{-1} Mpc^{-1}) shows no difference between the control and interacting samples at a 48% confidence level (see Table IV and Fig. 5). If anything, the sample of interacting galaxies possesses a median $M_B \sim 0.3$ mag *fainter* than the control samples. Due to the intrinsic errors involved in converting the interacting sample onto the B_T system, however, this small offset is probably neither reliable nor significant.

The distribution of Hubble types within each sample could also bias these results, since the type and strength of nuclear emission change systematically with Hubble type (cf. Stauffer 1982). Unfortunately this is not an easy effect to evaluate due to the chaotic morphologies of the sample of interacting galaxies. Beyond the fact that preference was given to disk-type galaxies, there is little that can be claimed regarding the exact distribution of pre-interaction spiral subtypes. There is some reason to believe that the interaction process might have the effect of modifying morphological type in the direction of later spiral subtypes, as Toomre (1981) has demonstrated tidal encounters to be capable of enhancing the wave patterns in spiral galaxies. For this reason, and because the morphological selection criteria should

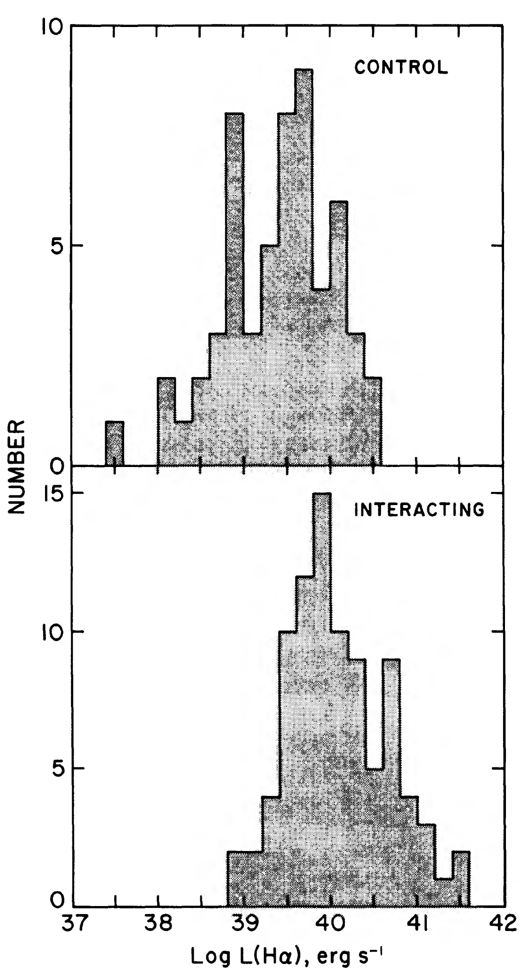

FIG. 4. Distribution of Hα luminosity for the interacting and isolated-galaxy samples.

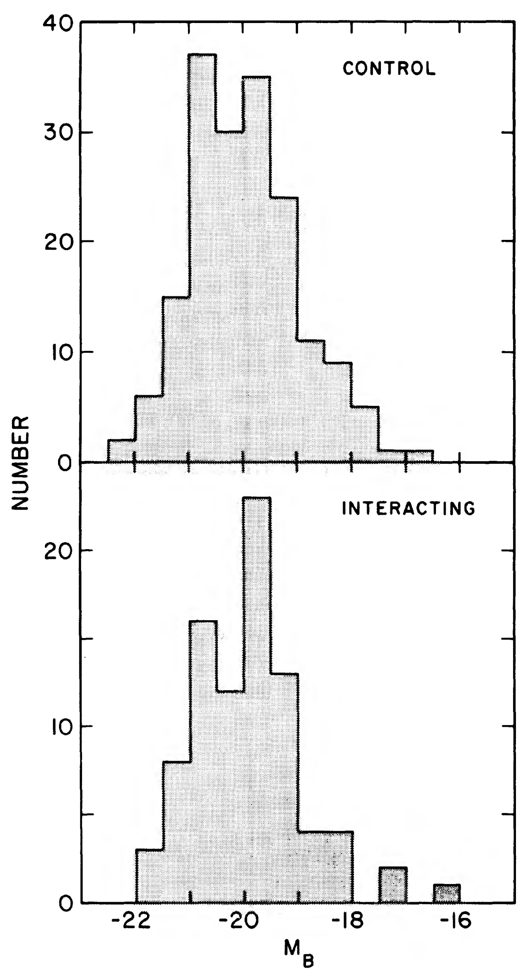

FIG. 5. Distribution of absolute magnitude for the interacting and combined isolated-galaxy samples.

have caused the selection of primarily disk-type galaxies, all isolated galaxies earlier than type S0 have been eliminated from the control samples. Inclusion of these objects would only strengthen the conclusions regarding enhanced activity in interacting systems, since most isolated galaxies earlier than type S0 have very low Hα luminosities and equivalent widths (see the surveys by Heckman, Balick, and Crane 1980; Stauffer 1982; and Keel 1983a).

Finally, a bias can occur in the nuclear emission properties due to a significant difference in the projected aperture sizes and therefore the sampling area of the different surveys. The median radial velocities and projected aperture diameters for the different samples are shown in Table IV. The median aperture size for the sample of interacting galaxies is over 2 kpc, which is more than three times the median size used in both the Stauffer and Keel isolated samples. Therefore a much larger portion of the galactic disk has been sampled in each system, which may lead to contamination of the nuclear properties. While Hα luminosity is expected to increase with aperture size, it is not at all clear exactly what effect this will have upon the observed Hα emission-line equivalent width. The increase in emission flux will be offset to some (unknown) degree by increased stellar Hα absorption from the surrounding disk.

As a means of obtaining some insight into this problem, I have compared the observed nuclear and global Hα equivalent widths for 43 spiral galaxies common to the surveys by Keel (1983a) and Kennicutt and Kent (1983). I find that the average ratio of global-to-nuclear Hα equivalent width increases quite smoothly from a value of ~ 0.4 in Sa-type galaxies, to ~ 1.0 in Sb's, and reaches ~ 2.5 in type Sc. Given the steady decrease in bulge-to-disk ratio along this same morphological sequence, this result is not surprising. If I were to assume, therefore, that the median morphological subtype for the sample of interacting galaxies were Sb, the increased aperture size used for this survey should have little or no effect upon the median Hα equivalent width. Even if I were to assume the extreme—that the sample of interacting galaxies is comprised mostly of Sc galaxies—the corresponding correction to the observed Hα equivalent widths would still give a median W_λ(Hα) a factor of ~ 2 larger than that for either of the control samples of isolated galaxies.

Furthermore, I find no obvious correlation between observed Hα equivalent width and distance (and therefore projected aperture size) for the sample of interacting galaxies (Fig. 6). This result offers further support to the belief that the excess in Hα equivalent width found for the interacting galaxies is not just an artifact of increased sampling area.

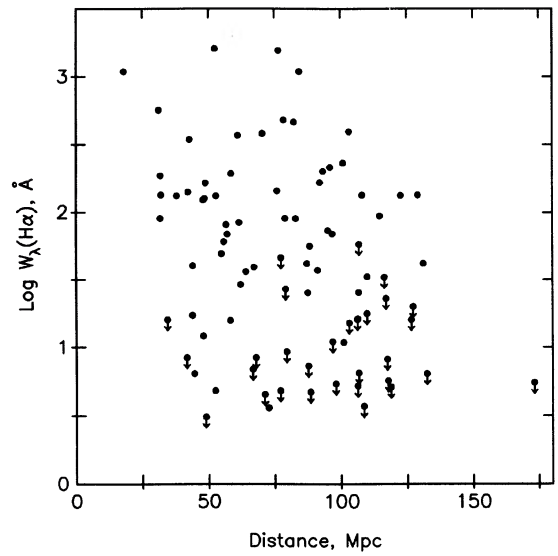

FIG. 6. Hα equivalent widths versus distance (on the scale described in Sec. II*c*) for the interacting galaxies; upper limits are marked by downward-facing arrows.

d) Correlations with Integral Properties

It has been suggested that correlations exist between pair separation and observed levels of star formation or radio activity in interacting systems (e.g., Stocke 1978; Hummel 1981; Karachentsev 1981; Tifft 1985). For this reason a search of parameter space involving M_B, L (Hα), W_λ(Hα), spectral class, pair separation, and nuclear colors has been made in an effort to reveal any such correlations that might exist within the sample of violently interacting galaxies. If we assume that the tidal force experienced by a galaxy is proportional to the mass ratio of the companion and parent galaxies, then it would also be interesting to look for correlations between either the mass or luminosity ratios of the pairs and the parameters mentioned above. Unfortunately there is not sufficient information available at this time pertaining to the mass or luminosity of the individual galaxies within the observed pairs in order to accomplish this. Furthermore, we expect that the interacting pairs in this sample are distributed fairly tightly about a mass ratio of one (see Sec. II*a*).

What at first appears to be a fairly strong correlation between M_B and L (Hα) turns out to be primarily a distance effect due to a decrease in sensitivity as the distance of the object increases. Further analysis of possible correlations between M_B and other properties of the interacting systems also yields a null result. I find no correlation of M_B with Hα emission-line equivalent width (Fig. 7), nor with spectral absorption or emission class.

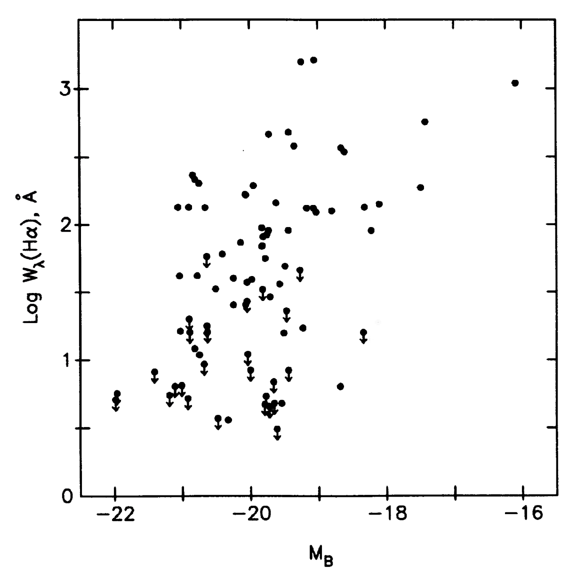

FIG. 7. Hα equivalent widths versus absolute magnitudes for the interacting galaxies; upper limits are marked by downward-facing arrows. Least-squares correlation coefficient = 0.40.

In order to investigate the effects of pair separation, I have constructed a separation index for the program galaxies. This separation index is defined to be the ratio of the combined semimajor-axis diameters of a galaxy pair and their projected separation (both measured from the POSS prints). High values of the index therefore represent galaxy pairs that have small projected separations relative to their total size. A value of exactly 1.0 corresponds to a pair of galaxies that would just make contact if their major axes were aligned.

The data show no significant relation between this separation index and either M_B, Hα equivalent width or luminosity, or spectral absorption or emission class of the individual components (Fig. 8). Remember, however, that these are severely disturbed galaxies that are the product of deep, interpenetrating collisions, and therefore most systems must have been at one time (and in some cases still are) in very close physical contact. Since they are now being observed in a post-collision situation, and therefore may already be receding from one another, their present separations are unlikely to correspond strongly with current or recent-past star-formation activity. Furthermore, we would expect the specifics of the reaction to depend upon many factors pertaining to the interaction event, such as the individual orbital characteristics, the mass ratio of the galaxy pair, and the availability of raw materials necessary for star formation, in addition to the physical proximity of the galaxies.

I have also synthesized approximate *UBV* colors from the observed spectra of the interacting galaxies. A comparison of these nuclear colors with Hα equivalent width and luminosity shows no trend in L (Hα) vs synthesized $U-B$ or $B-V$ color, but there is a strong correlation between Hα equivalent width and both $U-B$ and $B-V$ color (Fig. 9). This is to be expected since the colors and Hα equivalent width both primarily measure the same property of the stellar population, namely the ratio of young to old stars (cf. Huchra 1977).

Finally, a literature search for radio surveys that overlap the sample of interacting galaxies observed here has produced less than impressive results. Sulentic (1976) has surveyed the majority of systems in the Arp *Atlas of Peculiar Galaxies* at 2700 MHz with a detection limit of 60 mJy. Out of a total of 19 systems common to the two samples, only three were positively detected (UGC 4509, 8335, and 12099), and have an average radio luminosity of log L (2700) $\sim$ 22.7 W Hz^{-1}. Stocke *et al.* (1978) have also carried out a radio continuum survey of isolated pairs of galaxies from the catalog of Karachentsev (1972). In this survey, all four interacting systems in common between the two samples were detected (UGC 594, 8335, 9102, and 12914/15) and have an average radio luminosity of log L (2700) $\sim$ 21.5 W Hz^{-1}. These six systems detected in radio surveys span a wide range in Hα equivalent width, ranging from < 8.4 to 231 Å, and have Hα luminosities both above and below the median value for the whole sample. There is, therefore, no apparent correlation between the radio continuum luminosity and either the Hα equivalent width or luminosity of these interacting systems.

IV. DISCUSSION

a) Comparisons with Other Studies

Keel, Kennicutt, Hummel, and van der Hulst (1985; hereafter referred to as KKHH) recently completed a similar survey of the nuclear properties of an independent sample of

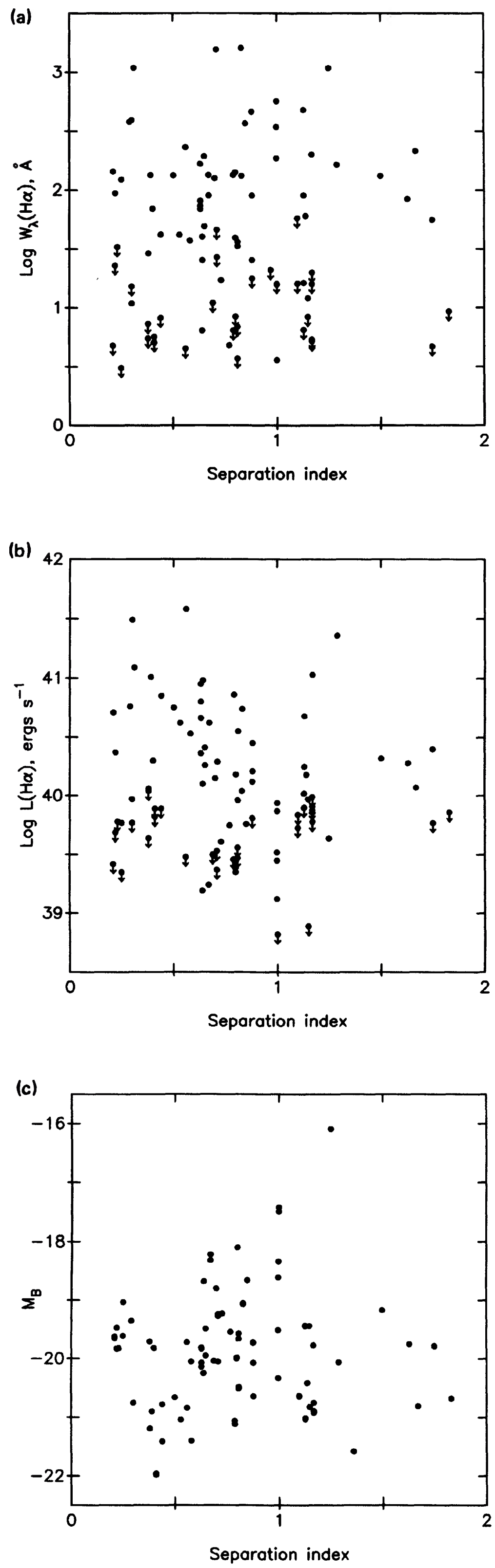

FIG. 8. (a) Hα equivalent widths versus separation index (see Sec. III*d*) for the interacting-galaxy sample. (b) Hα luminosities versus separation index for the interacting-galaxy sample. (c) M_B vs separation index for the interacting-galaxy sample.

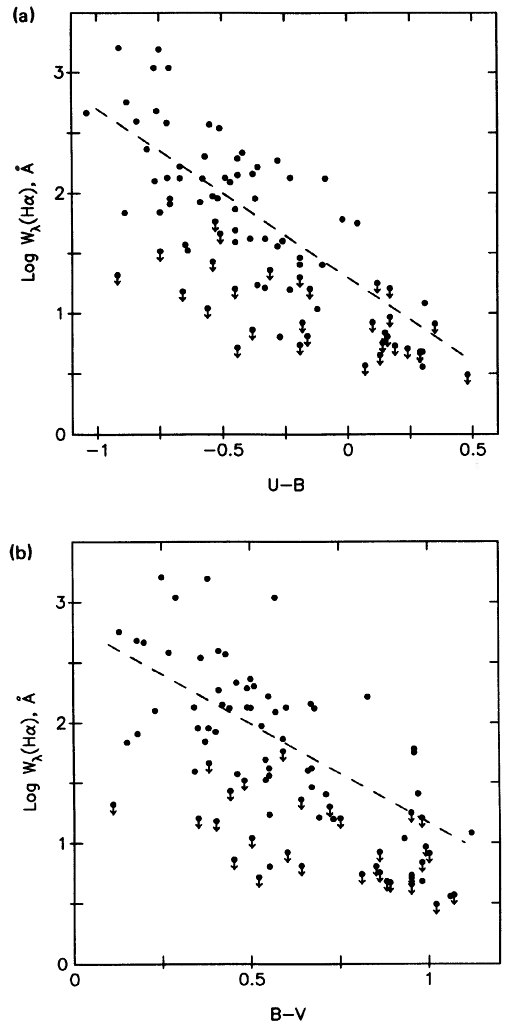

FIG. 9. (a) Hα equivalent widths versus synthesized $U-B$ colors for the interacting-galaxy nuclei; upper limits are marked by downward-facing arrows. The dashed line is a least-squares fit to the data (upper limits excluded). Least-squares correlation coefficient = 0.72. (b) Hα equivalent widths versus synthesized $B-V$ colors for the interacting-galaxy nuclei; upper limits are marked by downward-facing arrows. The dashed line is a least-squares fit to the data (upper limits excluded). Least-squares correlation coefficient = 0.64.

interacting galaxies. KKHH actually surveyed two somewhat distinct samples of interacting galaxies; a "complete" sample of spirals with close companions, based on projected separations and radial velocities, and an "Arp" sample of disturbed pairs.

The complete sample was drawn from an unpublished listing of probable pairs and groups from T. van Albada. This sample was selected independently of the appearance of the galaxies; many show no evidence of tidal distortion or structural peculiarity. The selection criteria for the Arp sample included sufficient angluar size to classify the galaxies, as well as evidence of tidal distortions, but not so severe that the galaxies were unrecognizable as spirals.

As with the present survey, KKHH also find a statistically significant excess in Hα emission-line luminosity and equivalent width for the interacting galaxies that they surveyed (see Table IV). They find median Hα equivalent widths of 28 and 24 Å for their complete and Arp samples, respectively. Compare these values with the median W_λ(Hα) ~40 Å found for the sample of violently interacting galaxies studied here. A comparison of Hα luminosities yields similar results. KKHH find median values of log L(Hα) of 39.0 and 40.2 (rescaled to $H_0 = 75$ km s^{-1} Mpc^{-1}) for their complete and Arp samples, respectively. The median log L(Hα) ~40.0 for the sample of violently interacting galaxies falls between these values.

At first glance, it would appear that, in spite of the wide range in level of star-forming activity found for the present sample of violently interacting galaxies, on the average this sample is in some respects even more burst-like than those surveyed by KKHH. As pointed out in the discussion of control samples, we must be careful to take into account the differences that exist between the present sample of violent interactors and those surveyed by KKHH. First, while the distribution in M_B is quite similar for the present sample and the KKHH complete sample, their Arp sample is ~0.5 mag more luminous (in the median) than the present sample. While this difference in median M_B could account to some extent for the observed increase in L (Hα) for the Arp sample, it does not explain the significantly larger median W_λ(Hα) found for the present sample of interacting galaxies.

A much more profound difference exists in the distribution of radial velocities (and therefore assumed distances) of objects in the various samples. The KKHH complete sample possesses a median radial velocity of only ~1700 km s^{-1}, while their Arp sample has a median of ~4900 km s^{-1}, and the present sample of interacting galaxies has a median radial velocity of ~7500 km s^{-1}. As discussed in the previous section, this change in median distance and therefore in the sampling area of the observed galaxies (KKHH also used 5 arcsec apertures for both samples) surely accounts for the differences in Hα luminosities, but does not fully explain the differences in Hα equivalent width. Notice, in this regard, that in spite of the fact that the KKHH Arp sample is more distant than their complete sample by almost a factor of 3, both have approximately the same median Hα equivalent width. Also recall that for the sample of violently interacting galaxies surveyed here, I find no dependence of W_λ (Hα) with distance. Furthermore, a comparison of the KKHH samples with systems from the present survey which occupy the same range in distance still shows a significant excess in W_λ (Hα).

The only remaining difference between the samples is in the type of objects selected. Except for some of the systems in the KKHH Arp sample, the majority of objects in their samples are physical pairs only and do not necessarily represent the kind of severe tidal interactions that the objects surveyed here are involved in. It is not unreasonable to assume, therefore, that a large part of the increase in observed Hα equivalent width found for the present sample of violently interacting galaxies is a result of the deeper, more interpenetrating collisions in which they are involved. But why then is there such a large fraction of systems with no detectable emission lines and spectral absorption features characteristic of an old, elliptical galaxy-like stellar population?

b) Comparison with Theoretical Models

One conceptual model that has received attention in the literature (cf. Joseph *et al.* 1984; KKHH) invokes the finite time scale of interactions to explain the wide range in nuclear and star-forming activity levels found in different samples of binary galaxies. In this picture the largest indirect effects of an interaction occur relatively early, when collisionally induced effects could raise star-formation rates by triggering the collapse of pre-existing molecular clouds or stimulate nuclear activity by dumping circumnuclear gas into a central engine.

The strongly interacting galaxies in this sample are being observed at later phases of the interaction (see Sec. II*a*) when the fuel for transient star formation and nuclear activity events may already be exhausted. While this model can explain post-burst systems that are dominated by an intermediate-age A–F type stellar population, it still fails to account for the many interacting galaxies that have very old stellar features (absorption class 1). To obtain spectral characteristics such as these requires that no significant star formation take place for several billion years—a length of time comparable to or even longer than the entire interaction process. These systems are not therefore simply "post-burst," but rather are "never-bursted."

This complete absence of recent star-formation activity in the central regions of many violently interacting galaxies implies either an initial lack of gas, or that gas is present but in inappropriate forms to support star formation. In response to the latter, Scalo and Struck-Marcell (1985) find the maximum star-formation rate to be very sensitive to the average mass density of gas near a critical density, and that incoherence and shear inhibition may also prevent star-formation bursts. On the other hand, results from high-resolution H I mapping of spiral galaxies show that a central depression in H I surface density is a common feature in late-type spiral galaxies (e.g., Shane 1980; Bosma 1981a,b; Bajaja and Shane 1982), which might imply a simple lack of fuel as the cause for the many non-star-forming systems.

Further support for this view may come from the results of narrowband Hα images which have been obtained for a subset of this sample of interacting galaxies. In several cases where there is a lack of nuclear star-formation activity there is a significant amount of star formation taking place in the outer disk regions of the galaxies. Sharp (1985) also finds that the Hα emission morphology of interacting systems seems to manifest itself primarily in one of two forms: (1) a strong central peak of emission at the nucleus in an otherwise smooth background, or (2) the emission is distributed either smoothly or lumpily throughout the entire galaxy. Therefore it appears that while sufficient fuel for supporting star formation may exist in the outer areas of some galaxies, the central regions are gas starved. This picture does not agree, however, with theoretical predictions that gas from the disk region of a galaxy will be transported to the nuclear regions during a tidal encounter (cf. White 1982; Norman and Silk 1983). If gas is being transported into the nucleus of these galaxies, it is evidently lacking an appropriate mechanism by which it is used to form stars or feed a central engine.

There is also the question of whether gas transfer is taking place between the galaxies in multiple systems. Of the 25 pairs for which I have obtained spectra of both galaxies, six ($\sim 25\%$) exhibit strikingly different spectral characteristics for the two components. In each case, one galaxy has H II region-like emission features indicating continuing star formation, while the other has either little or no detectable emission and an old, class 1-type stellar absorption spectrum indicating a lack of significant star formation for quite some time. There are also another four pairs (UGC 480, 2320, 4881, and Arp 250) that show no signs of recent star-formation activity in either of the two galaxies. It appears, therefore, that sometimes gas transfer between galaxies does not take place at all, and when it does it is often very one-sided in nature, fueling one galaxy at the expense of the other.

This apparent lack of fueling both within and between galaxies is also relevant to the production rate of active (i.e., Seyfert and LINER-like) nuclei in interacting systems. The results of this survey agree with those of KKHH for their Arp sample of interacting galaxies, and with Dahari (1985) for a sample of violently interacting galaxies that were selected from the *Atlas and Catalogue of Interacting Galaxies* (Vorontsov-Velyaminov 1959, 1977). Each of these samples shows a clear deficiency of active nuclei when compared to isolated systems. The KKHH complete sample, however, shows an increase in the occurrence of Seyfert nuclei, as do the less violently interacting members of Dahari's sample. KKHH suggest that the relatively early phases of interaction in which these less disturbed galaxies are involved may be conducive to the transport of disk gas into the nucleus to fuel a central engine.

The obvious corrollary to this hypothesis would then be that this inward flow of gas may be somehow restricted in the later phases of interaction due to either simple exhaustion of the supply or a disruption of the flow by the more severe and chaotic tidal forces experienced at this stage of the interaction. The previous discussion, however, indicates a surprising inefficiency of gas transport in many interacting systems throughout the *entire* course of the interaction process and not simply at later stages. KKHH also suggest an alternative approach in which the observable features of Seyfert and LINER nuclei are merely hidden by the onset of a large star burst. While this may be the case for the $\sim 20\%$ of the sample that have strong emission features, it would be very difficult to hide a typical Seyfert nucleus within the 30%–40% of the sample that have only very weak or no detectable emission lines. Perhaps collisions and Seyfert activity do not have a strict cause-and-effect relationship as previously supposed, but rather are semi-independent by-products of, for example, the deeper than normal potential wells that could be associated with multiple galaxy systems.

These results may also have implications for the hypothesis that galaxy-galaxy interactions are predominantly responsible for QSO phenomena. Stockton (1982) and de Robertis (1985), for example, set forth the assumption that, at least for some QSOs, an external means may be necessary to supply large amounts of metal-enriched gas, or to stimulate the transfer of gas already present, to incite activity. They link this external means with the interaction process. Previous discussion has shown, however, that gas transfer from one galaxy to another and from the outer regions to the nucleus of a galaxy can be very inefficient. Therefore one should exercise care when making the "common assumption" that an unknown mechanism exists through which gas provided by an interaction event is used to feed a central engine.

V. CONCLUSIONS

Optical spectrophotometry of the nuclear regions of 94 violently interacting spiral galaxies has shown:

(1) The nuclei exhibit a wide range in the level of optical line emission from ionized gas, but have a significantly high-

er overall level in both Hα equivalent width and luminosity than samples of field spirals.

(2) A surprisingly large fraction ($\sim 30\%$) of the nuclei are characterized by stellar absorption spectra reminiscent of old, elliptical galaxy-like stellar populations, and have only weak or no detectable emission lines.

(3) Fewer Seyfert and low-ionization nuclei are found than in isolated spirals. While galaxy-galaxy interactions *can* lead to enhanced levels of star-formation activity, this is not true in all cases. This survey provides examples of many systems that show no evidence of significant star formation over the past few billion years. While exhaustion of a galaxy's gas supply during the later phases of interaction can account for post-burst systems, it does not explain those galaxies that have experienced no significant star formation during a period of time equal to or even greater than the time scale of the entire interaction process.

The wide range in observed levels of star-formation activity might then be best explained by an equally large range in initial gas supplies in the central regions of the galaxies. Analysis of several pairs of interacting galaxies that contain one actively star forming and one inactive galaxy, as well as a few pairs in which both galaxies are inactive, indicates that gas transfer between galaxies does not always occur, and that when it does it is often very one-sided in nature. The spatial distribution of star formation within a few systems also indicates an inefficiency of radial gas transport within individual galaxies. Alternatively, gas may be present in the nuclear regions but is in inappropriate forms to support star formation. This conceptual model not only accounts for the general lack of star formation seen in the nuclear regions of many systems, but may also help explain the overall rarity of Seyfert nuclei in violently interacting galaxies.

I wish to thank my advisor Jay Gallagher for his advice and support throughout the course of this project, and I also thank Craig Foltz, Deidre Hunter, Bill Keel, and Nigel Sharp for valuable discussions. I also wish to thank the observing assistants and staff of the Steward Observatory for their help with the observations. Support from the University of Illinois Department of Astronomy for the observing time and the VIP data reduction and analysis system, and from the National Optical Astronomy Observatories in the form of a Graduate Research Assistantship, is also gratefully acknowledged.

REFERENCES

Adams, T. F. (1977). Astrophys. J. Suppl. **33**, 19.
Arp, H. C. (1966). *Atlas of Peculiar Galaxies* (California Institute of Technology, Pasadena); also in Astrophys. J. Suppl. **14**, 1.
Arp, H. C. (1982). Astrophys. J. **256**, 54.
Arp, H. C. (1983). Astrophys. J. **271**, 479.
Bajaja, E., and Shane, W. W. (1982). Astron. Astrophys. Suppl. **49**, 745.
Baldwin, J. A., Phillips, M. M., and Terlevich, R. (1981). Publ. Astron. Soc. Pac. **93**, 5.
Balick, B., and Heckman, T. M. (1982). Annu. Rev. Astron. Astrophys. **20**, 431.
Balkowski, C. (1973). Astron. Astrophys. **29**, 43.
Bosma, A. (1981a). Astron. J. **86**, 1791.
Bosma, A. (1981b). Astron. J. **86**, 1825.
Burstein, D., and Heiles, C. (1982). Astron. J. **87**, 1165.
Burstein, D., and Heiles, C. (1984). Astrophys. J. Suppl. **54**, 33.
Bushouse, H. A., and Gallagher, J. S. (1984). Publ. Astron. Soc. Pac. **96**, 273.
Condon, J. J. (1980). Astrophys. J. **242**, 894.
Condon, J. J., Condon, M. A., Gisler, G., and Puschell, J. J. (1982) Astrophys. J. **253**, 102.
Cutri, R. M., and McAlary, C. W. (1985). Astrophys. J. **296**, 90.
Dahari, O. (1984). Astron. J. **89**, 966.
Dahari, O. (1985). Astrophys. J. Suppl. **57**, 643.
de Robertis, M. (1985). Astron. J. **90**, 998.
de Vaucouleurs, G., de Vaucouleurs, A., and Corwin, H. (1976). *Second Reference Catalogue of Bright Galaxies* (University of Texas, Austin).
Ferland, G. J., and Netzer, H. (1983). Astrophys. J. **264**, 105.
Filippenko, A. V., and Greenstein, J. L. (1984). Publ. Astron. Soc. Pac. **96**, 530.
Fisher, J. R., and Tully, R. B. (1981). Astrophys. J. Suppl. **47**, 139.
Halpern, J. P., and Steiner, J. E. (1983). Astrophys. J. Lett. **269**, L37.
Heckman, T. M. (1980). Astron. Astrophys. **87**, 152.
Heckman, T. M., Balick, B., and Crane, P. C. (1980). Astron. Astrophys. Suppl. **40**, 295.
Huchra, J. P. (1980). Astrophys. J. Suppl. **35**, 171.
Hummel, E. (1980). Astron. Astrophys. **89**, L1.
Hummel, E. (1981). Astron. Astrophys. **96**, 111.
Hutchings, J. B., and Campbell, B. (1983). Nature **303**, 584.
Hutchings, J. B., Campbell, B., Crampton, D., Gower, A. C., and Morris, S. C. (1982). Astrophys. J. **262**, 48.
Joseph, R. D., Meikle, W. P. S., Robertson, N. A., and Wright, G. S. (1984). Mon. Not. R. Astron. Soc. **209**, 111.
Karachentsev, I. D. (1972). Commun. Special Astrophys. Obs. USSR **7**, 1.
Karachentsev, I. D. (1981). Pis'ma Astron. Zh. **7**, 1; Sov. Astron. Lett. **7**, 1.
Keel, W. C. (1983a). Astrophys. J. Suppl. **52**, 229.
Keel, W. C. (1983b). Astrophys. J. **269**, 466.
Keel, W. C. (1985). *Active Galaxies and Quasistellar Objects*, edited by J. S. Miller (University Science Books, Mill Valley, CA), p. 1.
Keel, W. C., Kennicutt, R. C., Hummel, E., and van der Hulst, J. M. (1985). Astron. J. **90**, 708.
Kennicutt, R. C. (1983). Astrophys. J. **272**, 54.
Kennicutt, R. C., and Kent, S. M. (1983). Astron. J. **88**, 1094.
Larson, R. B., and Tinsley, B. M. (1978). Astrophys. J. **219**, 46.
Morgan, W. W. (1958). Publ. Astron. Soc. Pac. **70**, 364.
Morgan, W. W. (1959). Publ. Astron. Soc. Pac. **71**, 394.
Morgan, W. W., and Mayall, N. U. (1957). Publ. Astron. Soc. Pac. **69**, 409.
Nilson, P. (1973). *Uppsala General Catalogue of Galaxies* (Uppsala Offset Center, Uppsala).
Norman, C., and Silk, J. (1983). Astrophys. J. **266**, 502.
Oke, J. B. (1974). Astrophys. J. Suppl. **27**, 21.
Osterbrock, D. E. (1985). *Structure and Evolution of Active Galactic Nuclei* (Osservatorio Astronomico di Trieste, Trieste) (in press).
Osterbrock, D. E., and Dahari, O. (1983). Astrophys. J. **273**, 478.
Philips, M. M., Charles, P. A., and Baldwin, J. A. (1983). Astrophys. J. **266**, 485.
Sandage, A. (1961). *The Hubble Atlas of Galaxies* (Carnegie Institution of Washington, Washington, DC).
Scalo, J. M., and Struck-Marcell, C. (1985). Preprint.
Schecter, P. L. (1980). Astron. J. **85**, 801.
Shane, W. W. (1980). Astron. Astrophys. **82**, 314.
Sharp, N. A. (1985). Poster paper, IAU Symposium No. 117.
Sharp, N. A., and Jones, B. F. (1980). Nature **283**, 275.
Shuder, J. M., and Osterbrock, D. E. (1981). Astrophys. J. **250**, 55.
Simkin, S. M., Su, H. J., and Schwarz, M. P. (1980). Astrophys. J. **237**, 404.
Smith, B. F., and Miller, R. H. (1982). In *International Kinematics and Dynamics of Galaxies*, IAU Symposium No. 100, edited by E. Athanassoula (Reidel, Dordrecht), p. 353.
Stauffer, J. R. (1982). Astrophys. J. Suppl. **50**, 517.

Stocke, J. T. (1978). Astron. J. **83**, 348.
Stockton, A. (1982). Astrophys. J. **257**, 33.
Sulentic, J. W. (1976). Astrophys. J. Suppl. **32**, 171.
Tift, W. G. (1985). Astrophys. J. **288**, 65.
Toomre, A. (1977). In *The Evolution of Galaxies and Stellar Populations*, edited by B. Tinsley and R. Larson (Yale University Observatory, New Haven), p. 401.
Toomre, A. (1981). In *The Structure and Evolution of Normal Galaxies*, edited by S. M. Fall and D. Lynden-Bell (University Press, Cambridge, England), p. 111.
Toomre, A., and Toomre, J. (1972). Astrophys. J. **178**, 623.
Vorontsov-Velyaminov, B. A. (1959). *Atlas and Catalogue of Interacting Galaxies*, Part I (Moscow State University, Moscow).
Vorontsov-Velyaminov, B. A. (1977). Astron. Astrophys. Suppl. **28**, 1.
White, S. D. M. (1982) In *Internal Kinematics and Dynamics of Galaxies*, IAU Symposium No. 100, edited by E. Athanassoula (Reidel, Dordrecht), p. 337.
Whitford, A. (1958). Astron. J. **63**, 201.